Hindawi
Mathematical Problems in Engineering
Volume 2017, Article ID 1985458, 11 pages
https://doi.org/10.1155/2017/1985458

Research Article

Upper-Bound Multi-Rigid-Block Solutions for Seismic Performance of Slopes with a Weak Thin Layer

Gang Zheng,[1,2,3] Xinyu Yang,[1,2] Haizuo Zhou,[1,2] Da Ha,[1,2] and Tianqi Zhang[1,2]

[1]*School of Civil Engineering, Tianjin University, Tianjin 300072, China*
[2]*Key Laboratory of Coast Civil Structure Safety of Ministry of Education, Tianjin University, Tianjin 300072, China*
[3]*State Key Laboratory of Hydraulic Engineering Simulation and Safety, Tianjin University, Tianjin 300072, China*

Correspondence should be addressed to Haizuo Zhou; zhzrobby@163.com

Received 17 July 2017; Accepted 22 October 2017; Published 26 November 2017

Academic Editor: Giovanni Garcea

The presence of a weak layer has an adverse influence on the seismic performance of slopes. The upper-bound solution serves as a rigorous method in the stability analysis of geotechnical problems. In this study, a multi-rigid-block solution based on the category of the upper-bound theorem of limit analysis is presented to examine the seismic performance of nonhomogeneous slopes with a weak thin layer. Comparison of the static factors of safety is conducted with various solutions (i.e., limit analysis with a different failure mechanism, limit equilibrium solution, and numerical method), and the results exhibit reasonable consistency. An analytical solution in estimating the critical yield acceleration coefficient is derived, and the influence of slope angle, slope height, and soil strength on the critical yield acceleration coefficient and failure mechanism is analyzed. Subsequently, Newmark's analytical procedure is employed to evaluate cumulative displacement with various real earthquake acceleration records as input motion. Results show that the strength and geometric parameters have a remarkable influence on the critical yield acceleration coefficient, and the cumulative displacement increases with the increasing slope angle.

1. Introduction

Extensive investigations have been conducted for the stability of slopes with homogeneous soil. However, the presence of a weak thin layer occurs often in practical engineering. This characteristic requires special attention from engineers with regard to the low shear strength of the weak layer, which has an adverse influence on the performance of slopes. Varying methodologies have been employed to estimate the static stability of slopes with a thin layer, including the limit equilibrium method (Fredlund and Krahn [1]), the upper-bound solution method (Huang and Song [2]), and finite element analysis (Griffiths and Marquez [3]; Ho [4]). However, few studies have focused on the seismic stability of nonhomogeneous slopes.

Many catastrophic slope failures have occurred because of earthquakes, such as the 2004 Chuetsu earthquake and the 2008 Wenchuan earthquake, highlighting the importance of addressing the seismic stability of slopes in geotechnical engineering practices. Once the damage of slopes occurs in urban area, a great number of economic losses may occur. The factor of safety of a slope, estimated using a pseudostatic approach, and the cumulative displacement, determined by adopting Newmark's sliding block method [5], are two commonly used tools to evaluate the seismic stability of slopes. The former provides a simple solution to evaluate the static stability (e.g., Seed et al. [6], Seed [7], and Chen [8]). The latter commonly adopts Newmark's sliding technique in estimating the cumulative displacement, which provides detailed information for the earthquake process. Compared with the pseudostatic approach, which underestimates the seismic stability (Ling et al. [9]; Michalowski [10]), Newmark's sliding technique helps to accurately evaluate the stability of slopes and can precisely determine effective reinforcements. Therefore, this method has recently been widely employed to slopes with a single layer of homogeneous

soil, with and without reinforcements (Chang et al. [11]; Ling et al. [9]; Ling and Leshchinsky [12]; Michalowski and You [13]; Li et al. [14]; He et al. [15]).

The extensions of the upper-bound solution to solving geotechnical problems have been explored by Chen [8]. The multi-rigid-block upper-bound solution is advantageous because it is conceptually clear and easily adopted and it satisfies the Mohr-Coulomb yield criterion (Michalowski [16]; Huang and Qin [17]; Huang and Song [2]). In this study, a three-rigid-block "classroom example" is first presented to show how to calculate the cumulative displacements, and a multi-rigid-block failure mechanism is then developed. The proposed failure mechanism is validated using previous studies with respect to the static factor of safety. The critical yield acceleration coefficient of an earth slope is evaluated by employing the pseudo-static method within the limit analysis framework. The influence of strength and geometric parameters on the critical yield acceleration coefficient is discussed. Subsequently, Newmark's analytical approach is employed to assess the cumulative displacement by considering different real earthquake acceleration records as input motion.

2. Upper-Bound Theorem

The method adopted is based on the kinematical theorem of limit analysis. The upper-bound theorem states that the rate of work done by external forces is less than or equal to the rate of energy dissipation in any kinematically admissible velocity field (Drucker et al. [18]). It can be expressed as

$$\int_S T_i v_i dS + \int_V X_i v_i dV \le \int_V \sigma_{ij}\, \dot{\varepsilon}_{ij}\, dV. \tag{1}$$

The first term on the left-hand side in (1) is the work rate of the unknown distributed load T_i on the loaded boundary S moving with the given velocity v_i. The second term on the left-hand side represents the work rate of the given distributed forces X_i in the kinematically admissible velocity v_i. The right-hand side is the rate of the internal work integrated over the entire volume V of the collapse mechanism.

Based on upper-bound solution, Michalowski and Drescher [19] proposed a class of three-dimensional rotational failure mechanism for the static stability of homogeneous slopes. This failure mechanism was further adopted for analyzing the static stability of slopes with reinforcement (Gao et al. [20]; Zhang et al. [21]; Yang et al. [22]). Different from the rotational failure mechanism for homogeneous slopes, the slip surface passes along the weak thin layer when a weak layer exists (Griffiths and Marquez [3]; Ho [4]) because the weak layer governs the failure mechanism. Huang et al. [23] originally developed a rotational-translational mechanism, which contains three rigid blocks, for a slope with a weak layer, as shown in Figure 1. The velocity of block b is v_b, and the angular velocities of block a and block c are ω_a and ω_c, respectively. An elaborate effort is required as the velocity discontinuities are bent at the interface between adjacent blocks. Zhou et al. [24] proposed a translational failure mechanism to examine the same issue. The rigid rotational blocks a and c in Huang et al.'s study were replaced by continuous deformation regions a and c, including a sequence of n rigid triangles.

3. Three-Block Failure Mechanism

To further establish the multiblock failure mechanism for nonhomogeneous slopes, a three-block failure mechanism acting as a "classroom example" is first presented. More blocks can be incorporated in the failure mechanism to improve the calculation accuracy. Figure 2 illustrates the three-block failure mechanism and velocity hodographs. Based on the normality rule, the direction of the velocities inclines with an angle φ with discontinuous surfaces, where φ is the friction angle of the soil in which the discontinuity surface lies. These velocities constitute a kinematically admissible velocity field. The ratio of the incipient velocities of each block is

$$\begin{aligned} \frac{v_b}{v_a} &= \frac{\sin\left(\theta_1 - 2\varphi_1 + \alpha_1 - \delta_w\right)}{\sin\left(\theta_1 - \varphi_1 - \varphi_2\right)} = A_a \\ \frac{v_c}{v_b} &= \frac{\sin\left(\varphi_1 + \varphi_2 - \delta_w + \alpha_2\right)}{\sin\left(\theta_2 - 2\varphi_1\right)} = A_c, \end{aligned} \tag{2}$$

where v_a, v_b, and v_c are the incipient velocities in different blocks, ABCG, CDFG, and DEF, respectively, and φ_1 and φ_2 are the internal friction angles of the soils, respectively. The angles of θ_1, θ_2, α_1, α_2, and δ_w are illustrated in Figure 2.

For the assumed kinematically admissible failure mechanism, once the rates of work performed by the external forces and the self-weight of soils exceed the energy dissipation rate, the soil will reach its limit state. The rate of external work due to the self-weight of soils can be calculated as follows:

$$\begin{aligned} W^{\gamma} = W_a{}^{\gamma} + W^{\gamma}{}_b + W_c{}^{\gamma} = g\left[m_a \sin\left(\alpha_a - \varphi_1\right) v_a \right. \\ \left. + m_b \sin\left(\delta_w - \varphi_2\right) v_b - m_c \sin\left(\alpha_c - \varphi_1\right) v_c\right], \end{aligned} \tag{3}$$

where m_a, m_b, and m_c are the masses of different blocks and g is the gravitational acceleration.

Once the earth slope is subjected to horizontal earthquakes, the rate of the inertial force should be considered in the energy balance equation. According to previous investigations (Li et al. [14]; He et al. [15]), the effect of the failure mechanism on the shaking mode can be neglected. The influences of the horizontal earthquakes acting on the collapse mass are evaluated by horizontal forces applied to the center of soil mass, which can be calculated as follows:

$$\begin{aligned} W^s = W_a^s + W_b^s + W_c^s = kg\left[m_a v_a \cos\left(\alpha_a - \varphi_1\right)\right. \\ \left. + m_b v_b \cos\left(\delta_w - \varphi_2\right) - m_c v_c \cos\left(\alpha_c - \varphi_1\right)\right]. \end{aligned} \tag{4}$$

The rate of internal energy dissipation D^c is induced by soil cohesion in the collapse mechanism. Energy dissipation is calculated as the sum of the rates of dissipation along the discontinuity surfaces, and the blocks move in directions

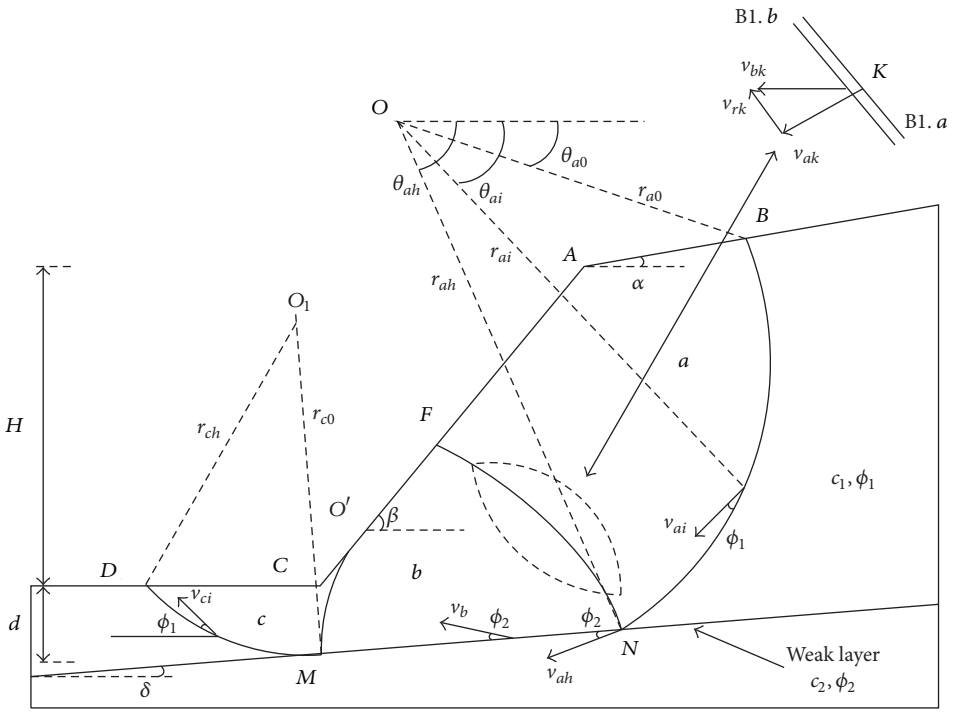

Figure 1: Rotational-translational mechanism (after Huang et al. 2013 [23]).

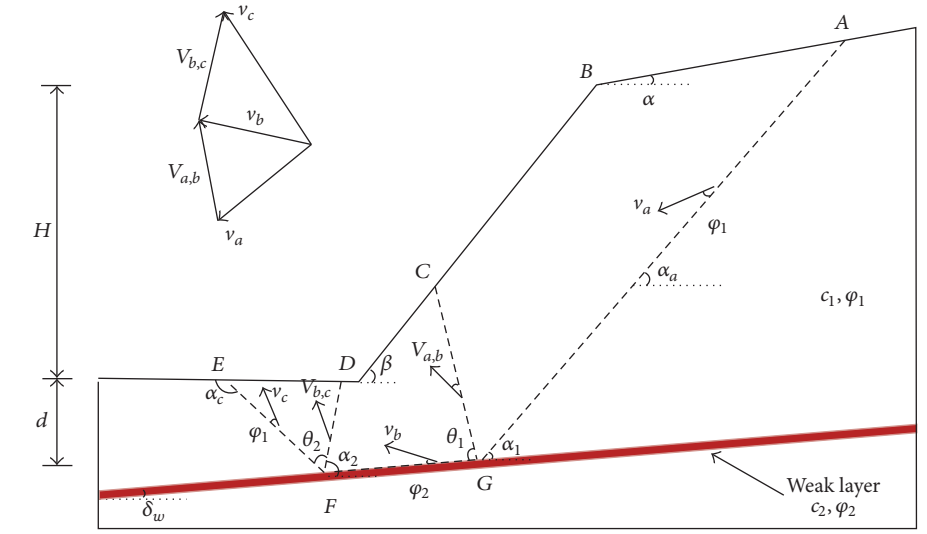

Figure 2: Three-block failure mechanism for slopes with a weak layer.

that make an angle φ_1 or φ_2 with the discontinuity surfaces. The energy dissipation along the discontinuity surfaces is the soil cohesion multiplied by the relative velocities and the length of discontinuity surface in the soil mass.

To determine the critical yield acceleration coefficient k_c, at which the slope will be at the limit state, the k_c value can be calculated by equating the rate of internal energy dissipation to the external rate of work.

$$W^{\gamma} + W^{s} = D^{c}. \tag{5}$$

The critical yield acceleration coefficient k_c can be evaluated as

$$k_c = \frac{D^c - W^{\gamma}}{g\left[m_a v_a \cos\left(\alpha_a - \varphi_1\right) + m_b v_b \cos\left(\delta_w - \varphi_2\right) - m_c v_c \cos\left(\alpha_c - \varphi_1\right)\right]}. \tag{6}$$

Newmark's sliding block technique, which was used in a previous study in investigating the performance of slopes under the rotational failure mechanism in both two- and three-dimensional problems (e.g., Chang et al. [11], Li et al. [14], and He et al. [15]), was employed for estimating the cumulative displacement of slopes. The sliding block begins to accelerate with acceleration values $\ddot{u}_a$, $\ddot{u}_b$, and $\ddot{u}_c$; thus, balancing the work rate equation yields

$$W^{\gamma} + k_c g \left[m_a v_a \cos(\alpha_a - \varphi_1) + m_b v_b \cos(\delta_w - \varphi_2) - m_c v_c \cos(\alpha_c - \varphi_1) \right] = D^c + m_a v_a \ddot{u}_a + m_b v_b \ddot{u}_b + m_c v_c \ddot{u}_c. \tag{7}$$

According to Newmark's analytical approach (Newmark [5]), the downhill movement of soil was assumed. The direction of soil displacement is not influenced by the direction of the earthquake acceleration. Earthquake acceleration varies during the whole process of shaking. The velocity of the failing masses increases from zero during the time interval when the seismic coefficient k exceeds the critical yield acceleration coefficient k_c of earth slopes. Based on Newmark's analytical approach [5], the cumulative displacement can be estimated by integrating the velocity of the failing soil masses, which can be integrated by acceleration. Note that the acceleration herein is a real acceleration rather than the time derivative of the incipient velocity. Subtracting (6) from (7), the acceleration can be expressed as

$$g(k - k_c) \left[m_a \cos(\alpha_a - \varphi_1) \frac{v_a}{v_b} + m_b \cos(\delta_w - \varphi_2) - m_c \cos(\alpha_c - \varphi_1) \frac{v_c}{v_b} \right] = \ddot{u}_b \left(m_a \frac{v_a}{v_b} \frac{\ddot{u}_a}{\ddot{u}_b} + m_b + m_c \frac{v_c}{v_b} \frac{\ddot{u}_c}{\ddot{u}_b} \right). \tag{8}$$

To satisfy the kinematical admissibility, the ratios of $\ddot{u}_{ah}/\ddot{u}_b$ and $\ddot{u}_b/\ddot{u}_{c0}$ are the same as v_{ah}/v_b and v_b/v_{c0} (Michalowski and You [13]). This behavior occurs because the deformation of soil is governed by the normality rule. Therefore, the acceleration $\ddot{u}_b$ can be expressed as

$$\ddot{u}_b = g(k - k_c) \frac{m_a \cos(\alpha_a - \varphi_1) A_a + m_b \cos(\delta_w - \varphi_2) - m_c \cos(\alpha_c - \varphi_1) A_c}{m_a A_a^2 + m_b + m_c A_c^2} = g(k - k_c) C. \tag{9}$$

Coefficient C can be evaluated by the proposed translational mechanism. Additionally, the slope geometries and soil properties are contained in coefficient C, which is involved in the optimization of the proposed collapse mechanism. The horizontal displacement in the toe of slopes can be determined through the analysis of the displacement of any point in the failing soil masses:

$$u_{b(x)} = \cos(\delta_w - \varphi_2) \int_t \int_t \ddot{u}_b dt\, dt = C \cos(\delta_w - \varphi_2) \int_t \int_t g(k - k_c)\, dt\, dt. \tag{10}$$

Integration is made over time, which only includes intervals for which the initial integral is positive. The coefficient C is related to the geometry of the structure, the soil condition, and the failure mechanism.

4. Multiblock Failure Mechanism

A multiblock failure mechanism was further employed based on the previous three-block collapse mechanism. Figure 3 shows the multiblock failure mechanism in which the blocks ABCD and DEF in the three-block failure mechanism are divided into a sequence of discrete blocks. The relations between the incipient velocities of different blocks can be expressed as follows:

$$\begin{aligned}
\frac{v_{a,i}}{v_{a,1}} &= \frac{\ddot{u}_{a,i}}{\ddot{u}_{a,1}} = \prod_{k=2}^{k=i} \frac{\sin(\theta_{a,k} - 2\varphi_1 + \alpha_{a,k-1} - \alpha_{a,k})}{\sin(\theta_{a,k} - 2\varphi_1)} = A_{a,i} \\
\frac{v_{c,i}}{v_{c,1}} &= \frac{\ddot{u}_{c,i}}{\ddot{u}_{c,1}} = \prod_{k=2}^{k=i} \frac{\sin(\theta_{c,k} - 2\varphi_1 + \alpha_{c,k-1} - \alpha_{c,k})}{\sin(\theta_{c,k} - 2\varphi_1)} = A_{c,i} \\
\frac{v_b}{v_{a,n}} &= \frac{\ddot{u}_b}{\ddot{u}_{a,n}} = \frac{\sin(\theta_b - 2\varphi_1 + \alpha_{a,n} - \delta_w)}{\sin(\theta_b - \varphi_1 - \varphi_2)} = A_{a,b} \\
\frac{v_{c,1}}{v_b} &= \frac{\ddot{u}_{c,1}}{\ddot{u}_b} = \frac{\sin(\varphi_1 + \varphi_2 - \delta_w + \alpha_{c,1})}{\sin(\theta_{c,1} - 2\varphi_1)} = A_{b,c},
\end{aligned} \tag{11}$$

where $i = 2, 3, 4, \ldots, n$ and $k = 2, 3, 4, \ldots, i$ and $v_{a,i}$ and $v_{c,i}$ are the velocities of blocks ABCD and DEF, respectively.

The rate of external work due to the self-weight of soils can be estimated as follows:

$$W^{\gamma} = \sum_{i=1}^{n} m_{a,i} v_{a,i} \sin(\alpha_{a,i} - \varphi_1) + m_b v_b \sin(\delta_w - \varphi_2) - \sum_{i=1}^{n} m_{c,i} v_{c,i} \sin(\alpha_{c,i} - \varphi_1). \tag{12}$$

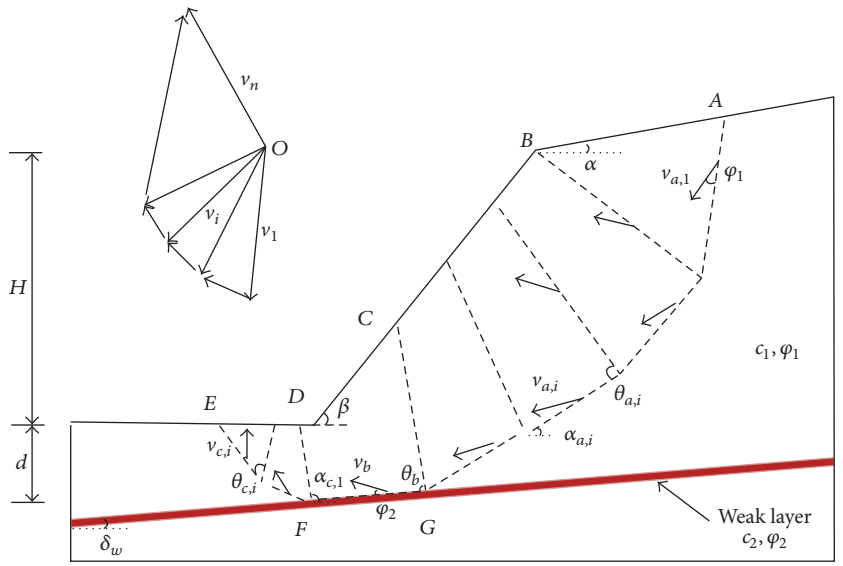

FIGURE 3: Multiblock failure mechanism for slopes with a weak layer.

The effects of the horizontal earthquakes can be evaluated as follows:

$$W^s = kg\left[\sum_{i=1}^{n} m_{a,i} v_{a,i} \cos\left(\alpha_{a,i} - \varphi_1\right) + m_b v_b \cos\left(\delta_w - \varphi_2\right) - \sum_{i=1}^{n} m_{c,i} v_{c,i} \cos\left(\alpha_{c,i} - \varphi_1\right)\right]. \tag{13}$$

The rate of internal energy dissipation D^c is estimated as the sum of the rates of dissipation along the discontinuity surfaces in the multiblock failure mechanism. The critical yield acceleration coefficient k_c can be evaluated as

$$k_c = \frac{D^c - W^\gamma}{\sum_{i=1}^{n} m_{a,i} g v_{a,i} \cos\left(\alpha_{a,i} - \varphi_1\right) + m_b g v_b \cos\left(\delta_w - \varphi_2\right) - \sum_{i=1}^{n} m_{c,i} g v_{c,i} \cos\left(\alpha_{c,i} - \varphi_1\right)}. \tag{14}$$

An additional term induced by inertial forces acting on the failing soil masses when the earthquake acceleration of the ground motion exceeds the critical acceleration of the structure is as follows:

$$W^\gamma + kg\left[\sum_{i=1}^{n} m_{a,i} v_{a,i} \cos\left(\alpha_{a,i} - \varphi_1\right) + m_b v_b \cos\left(\delta_w - \varphi_2\right) - \sum_{i=1}^{n} m_{c,i} v_{c,i} \cos\left(\alpha_{c,i} - \varphi_1\right)\right] = D^c + \sum_{i=1}^{n} m_{a,i} v_{a,i} \ddot{u}_{a,i} + m_b v_b \ddot{u}_b + \sum_{i=1}^{n} m_{c,i} v_{c,i} \ddot{u}_{c,i}. \tag{15}$$

Therefore, the acceleration $\ddot{u}_b$ in the multiblock failure mechanism can be expressed as

$$\ddot{u}_b = g\left(k - k_c\right) \frac{\sum_{i=1}^{n} m_{a,i} v_{a,i} \cos\left(\alpha_{a,i} - \varphi_1\right) + m_b v_b \cos\left(\delta_w - \varphi_2\right) - \sum_{i=1}^{n} m_{c,i} v_{c,i} \cos\left(\alpha_{c,i} - \varphi_1\right)}{\sum_{i=1}^{n} m_{a,i} v_{a,i} \ddot{u}_{a,i} + m_b v_b \ddot{u}_b + \sum_{i=1}^{n} m_{c,i} v_{c,i} \ddot{u}_{c,i}} = g\left(k - k_c\right) C. \tag{16}$$

The above expression indicates that acceleration of a failing structure affects the failure mechanism and the critical yield acceleration coefficient k_c. The double integral in (10) is needed to be introduced when calculating the displacement.

5. Validation

To validate the proposed multi-rigid-block upper-bound analysis, two well-defined classical slopes with a weak thin

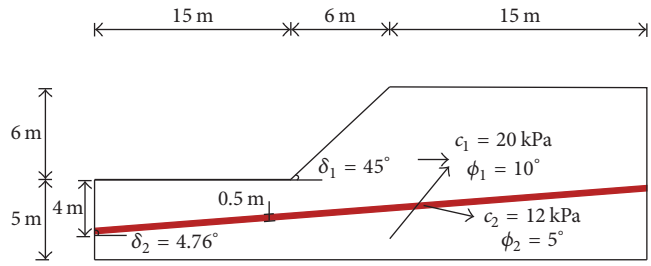

Figure 4: Schematic diagram of slope A.

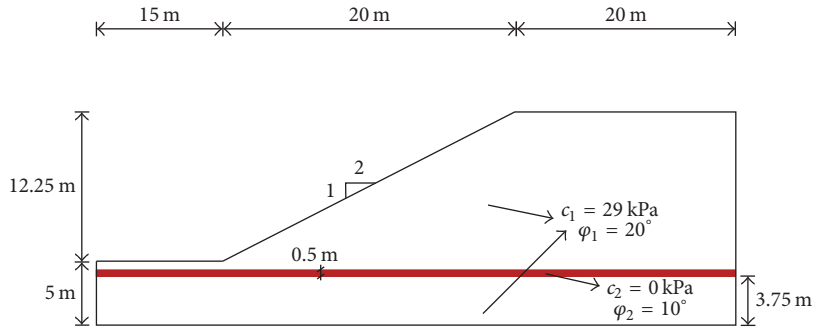

Figure 5: Schematic diagram of slope B.

layer were selected in calculating the static factor of safety. Figure 4 illustrates the schematic diagram of slope A (Huang et al. [23]). A nonhomogeneous slope A has an angle $\beta = 45^\circ$ and height $H = 6$ m. The soil strength parameters of slopes were $\varphi_1 = 10^\circ$, $c_1 = 20$ kPa, and a 0.5 m thick weak layer characterized by $\varphi_2 = 5^\circ$ and $c_2 = 12$ kPa. Figure 5 shows the geometric and strength parameters of a nonhomogeneous slope B underlain by a thin weak layer, which was previously analyzed by Fredlund and Krahn [1]. A 1 : 2 slope has a height of $H = 12.25$ m, with soil properties of $\varphi_1 = 20^\circ$ and $c_1 = 29$ kPa and strength parameters of the weak layer of $\varphi_2 = 10^\circ$ and $c_2 = 0$ kPa.

The factor of safety computed by the proposed multi-rigid-block failure mechanism for slope A was first compared with the results obtained by Huang et al. [23] and Zhou et al. [24], as shown in Figure 6. The calculated factor of safety from the multi-rigid-block failure mechanism was equal to the FEM result. The value was slightly higher than the result from Discontinuity Layout Optimization (Zhou et al. [24]) and the upper-bound solution based on the rotational-translational collapse mechanism (Huang et al. [23]), but it was better than that of the upper-bound solution based on the translational collapse mechanism. Figure 7 shows the validation of the factor of safety between the upper-bound multi-rigid-block failure mechanism and the results obtained by Fredlund and Krahn [1] and Zhou et al. [24]. Fredlund and Krahn [1] adopted Spencer's method and Janbu's rigorous method to evaluate the stability of slope B. The proposed multi-rigid-block failure mechanism yields a factor of safety of 1.34, which is in the vicinity of that between the DLO and analytical solutions. The comparison demonstrated the reasonable consistency with previous studies. The proposed

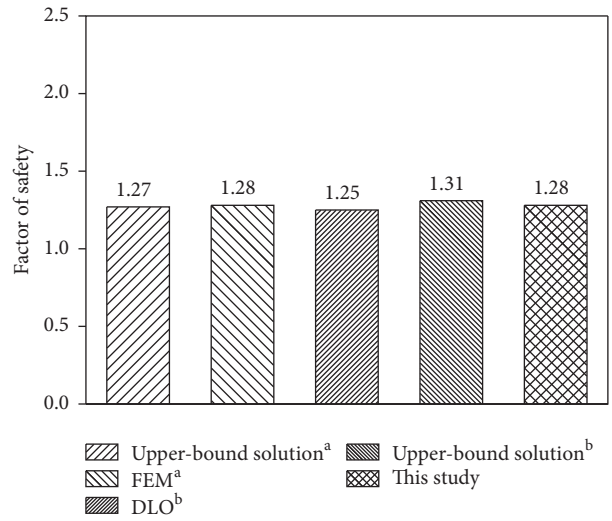

Figure 6: Validation of the results of the static factor of safety (slope A). a: Huang et al. [23]; b: Zhou et al. [24].

multi-rigid-block failure mechanism was then employed to examine the critical yield acceleration coefficient and cumulative displacements of the slopes.

6. Critical Yield Acceleration Coefficient

Before evaluating the cumulative displacement under earthquake load, the influence of geometric and strength parameters on critical yield acceleration coefficient was analyzed. This coefficient is the threshold at which the displacement of slopes starts accumulating.

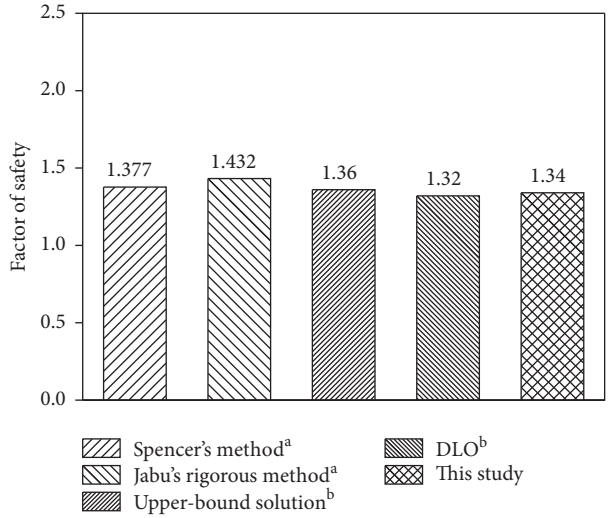

Figure 7: Validation of the results of the static factor of safety (slope B). a: Huang et al. [23]; b: Zhou et al. [24].

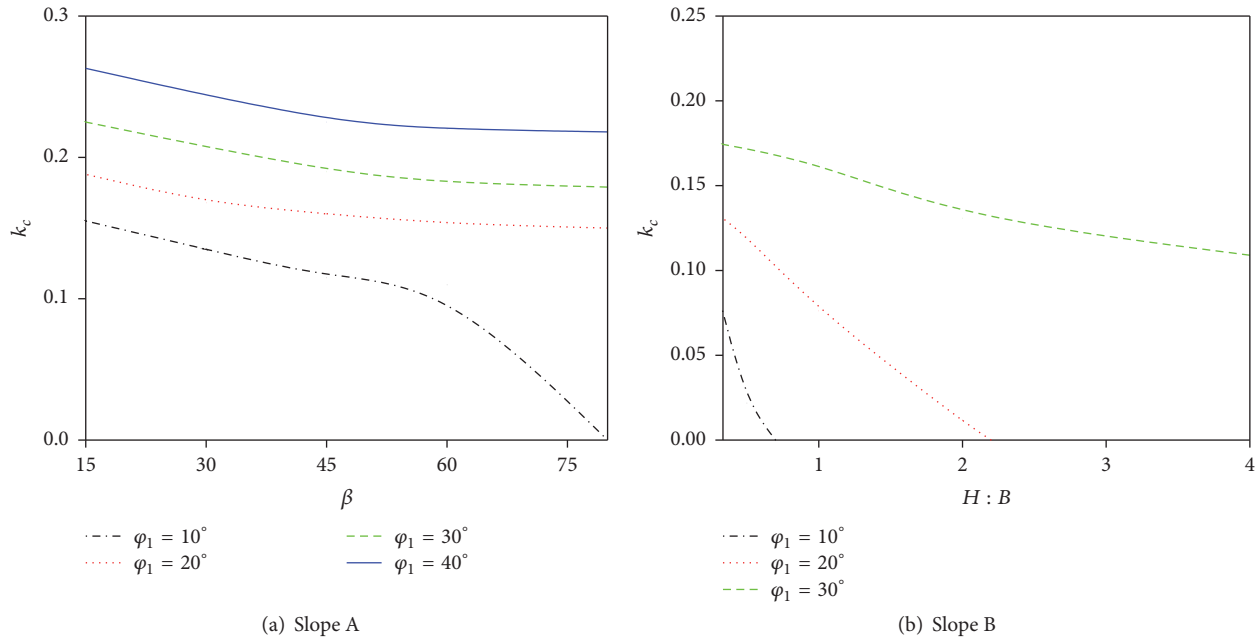

(a) Slope A (b) Slope B

Figure 8: Critical yield acceleration coefficient with various slope angles.

Figures 8, 9, and 10 show the critical yield acceleration coefficients of slopes A and B for various angles, slope heights (H), and depths of the weak layer (d), respectively. Ranges of slope angles ($\beta = 15^\circ$–90°) and frictional strength ($\varphi = 10^\circ$–40°) were analyzed for slope A, whereas slope inclinations of 0.5 : 1 to 4 : 1 and friction angles of $\varphi = 10^\circ$–30° were estimated for slope B. As expected, the critical yield acceleration coefficient k_c decreased with the increasing slope angle and slope height, but it increased with the increasing depth of the weak layer. Slope A was more stable than slope B based on the calculated critical yield acceleration coefficient k_c.

Figure 11 presents the critical yield acceleration coefficients of slopes A and B for various soil strengths. A reduction factor R (defined as $R = c_2/c_1 = \tan\varphi_2/\tan\varphi_1$) was introduced here to show the effect of the soil strength of the weak layer on k_c value. It is a homogeneous slope when R is equal to 1.0. Generally, the critical yield acceleration coefficient k_c increased with φ_1 and R. Note that there was a critical R value existing in slope A, indicating increased R was not beneficial to the k_c value as the collapse mechanism changed to a rotational log-spiral failure mode. Critical R value of slope A is greater than that of slope B because the angle of slope A is larger than that of slope B, indicating the rotational log-spiral failure is likely to occur.

Figures 12 and 13 illustrate the potential failure mechanism for various friction angles of slope A and slope B at the critical yield acceleration coefficient k_c, respectively.

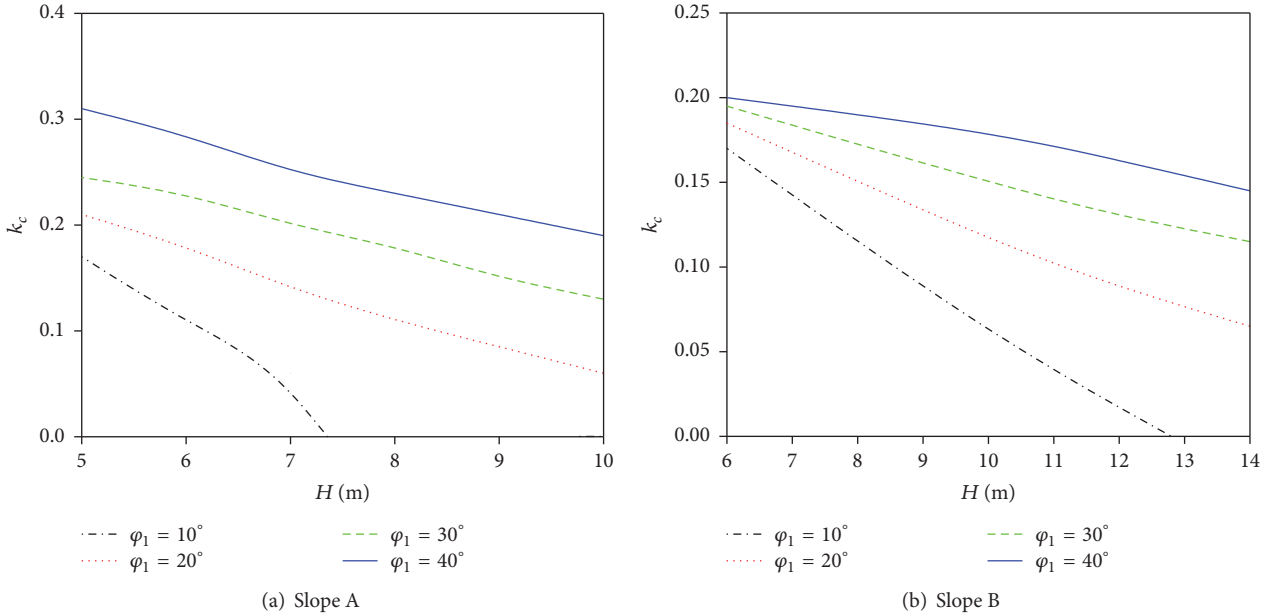

(a) Slope A (b) Slope B

Figure 9: Critical yield acceleration coefficient with various slope heights.

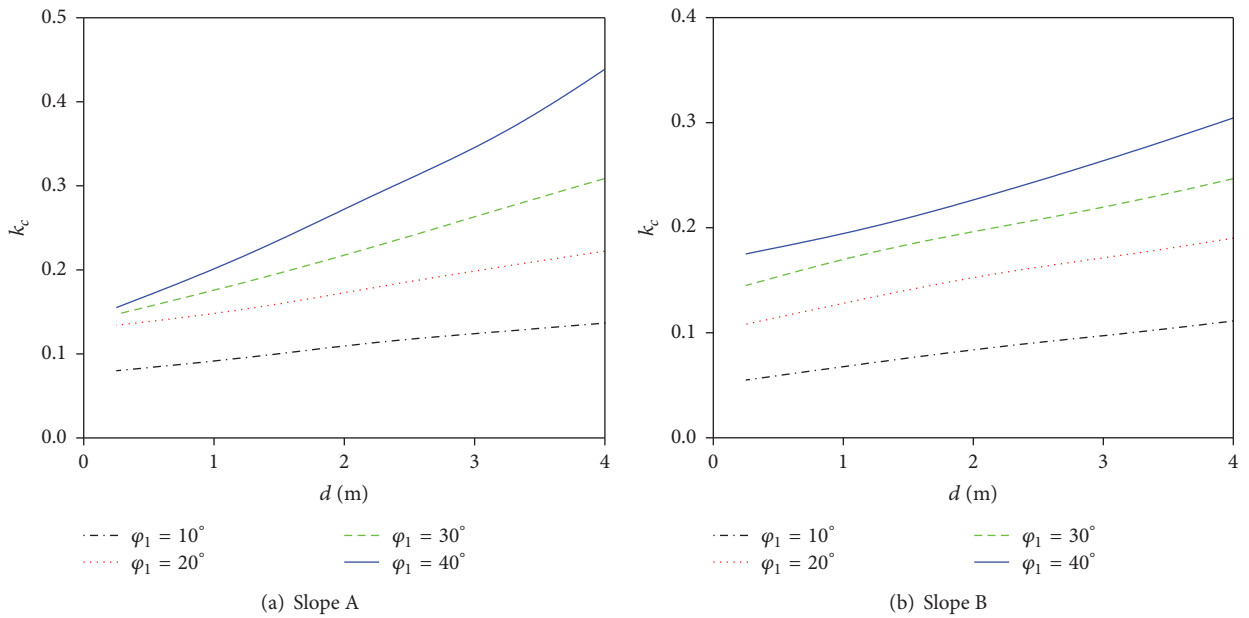

(a) Slope A (b) Slope B

Figure 10: Critical yield acceleration coefficient with various depths of the weak layer.

A panhandling failure mechanism partially penetrating the weak layer can be identified in both slopes A and B. For slope A, the failure slip significantly increased when the friction angle was higher than 20° compared with slope B. This behavior is due to the inclination of the weak thin layer, which tends to be mobilized in large landslides.

7. Cumulative Displacements

The cumulative displacements of slopes with a weak thin layer were calculated through Newmark's analytical approach. The real earthquake motion input has a significant effect on the cumulative displacements of the failing soil masses. Therefore, different real earthquake acceleration records were selected to evaluate the cumulative displacements of slopes. Following He et al. [15], three typical earthquake records were adopted. Figure 14(a) shows the Imperial Valley-06 earthquake records, with a peak earthquake acceleration (PGA) of 0.307 g and a record duration of 14.76 s. Figure 14(b) shows the Kobe earthquake record, with PGA = 0.345 g and a record duration of 20 s. Figure 14(c) illustrates the Parkfield-02 earthquake record, with PGA = 0.373 g and a

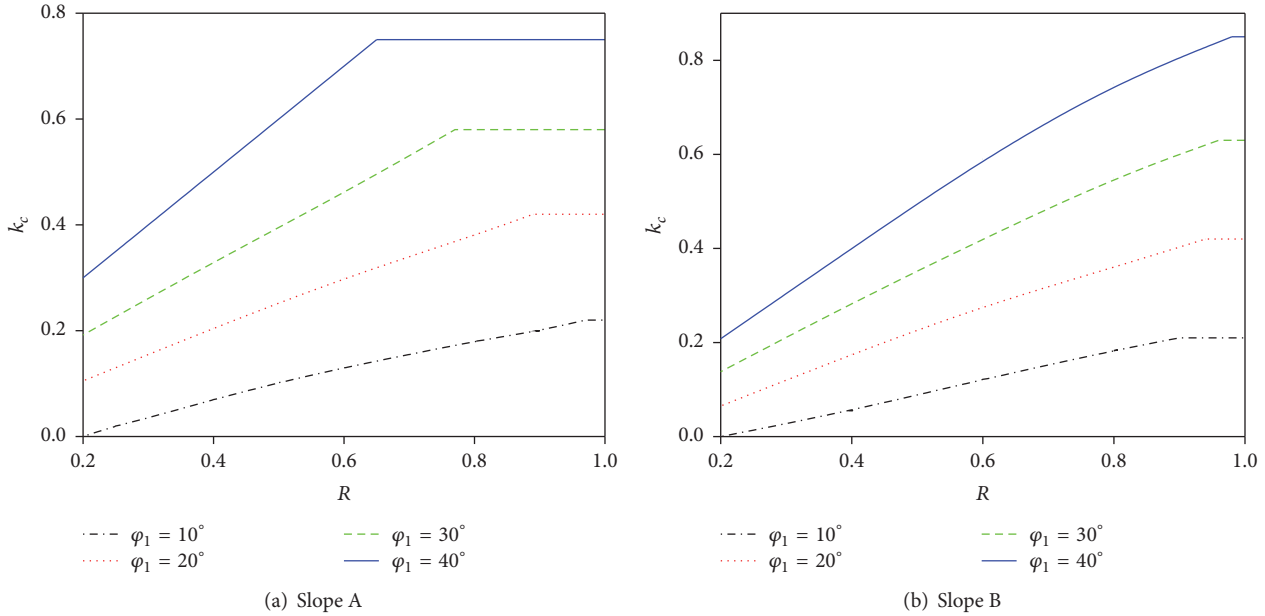

Figure 11: Critical yield acceleration coefficient with various strengths of weak clay.

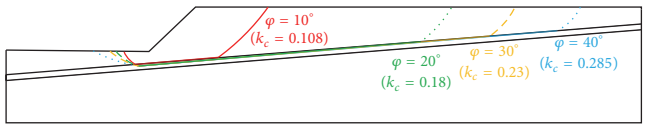

Figure 12: Failure mechanism for various friction angles of slope A at the critical yield acceleration coefficient k_c.

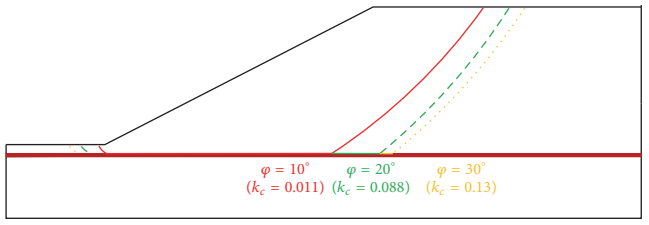

Figure 13: Potential failure mechanism for various friction angles of slope B at the critical yield acceleration coefficient k_c.

duration of 21.07 s. The constant time intervals of the Imperial Valley-06 and Kobe earthquake records are 0.01 s, whereas the constant time interval of the Parkfield-02 earthquake record is 0.005 s. These earthquake records were used to assess the performance of the slopes with varying slope angles subjected to seismic loads. Tables 1 and 2 list the seismic displacements of slope A and slope B with various slope angles. The maximum horizon displacements of the slopes increased with increasing peak earthquake acceleration of the earthquake motion input. In addition, the cumulative displacement significantly increased with the slope angles. Thus, special attention should be paid to steep slopes in engineering applications.

8. Conclusions

In this investigation, the seismic performance of slopes with a weak layer is estimated. Based on the upper-bound solution, a three-rigid-block acting as a "classroom example" is first presented, and then a multi-rigid-block failure mechanism is further proposed. The static factor of safety calculated by the proposed method exhibits strong agreement with previous studies. Subsequently, two well-defined cases existing in the available literature are introduced to analyze the influence of soil conditions and geometric parameters on the critical yield acceleration coefficient. Newmark's analytical procedure is adopted to assess the cumulative displacement. The results show that the failure slip is greatly deepened when the weak thin layer is inclined. The critical yield acceleration coefficient increased with soil strength and depth of the weak layer and decreased with slope angle and slope height. The cumulative displacement of the slope increased significantly with the peak earthquake acceleration. Lastly, the slope angle has a prominent effect on the seismic performance of structures. Note that two-dimensional analysis results in a conservative solution in comparison to three-dimensional method (Tanchaisawat et al. [25]; Ho [26]). Thus, future work will be conducted on the seismic performance of slopes with a weak layer using three-dimensional analysis.

Conflicts of Interest

The authors declare that they have no conflicts of interest.

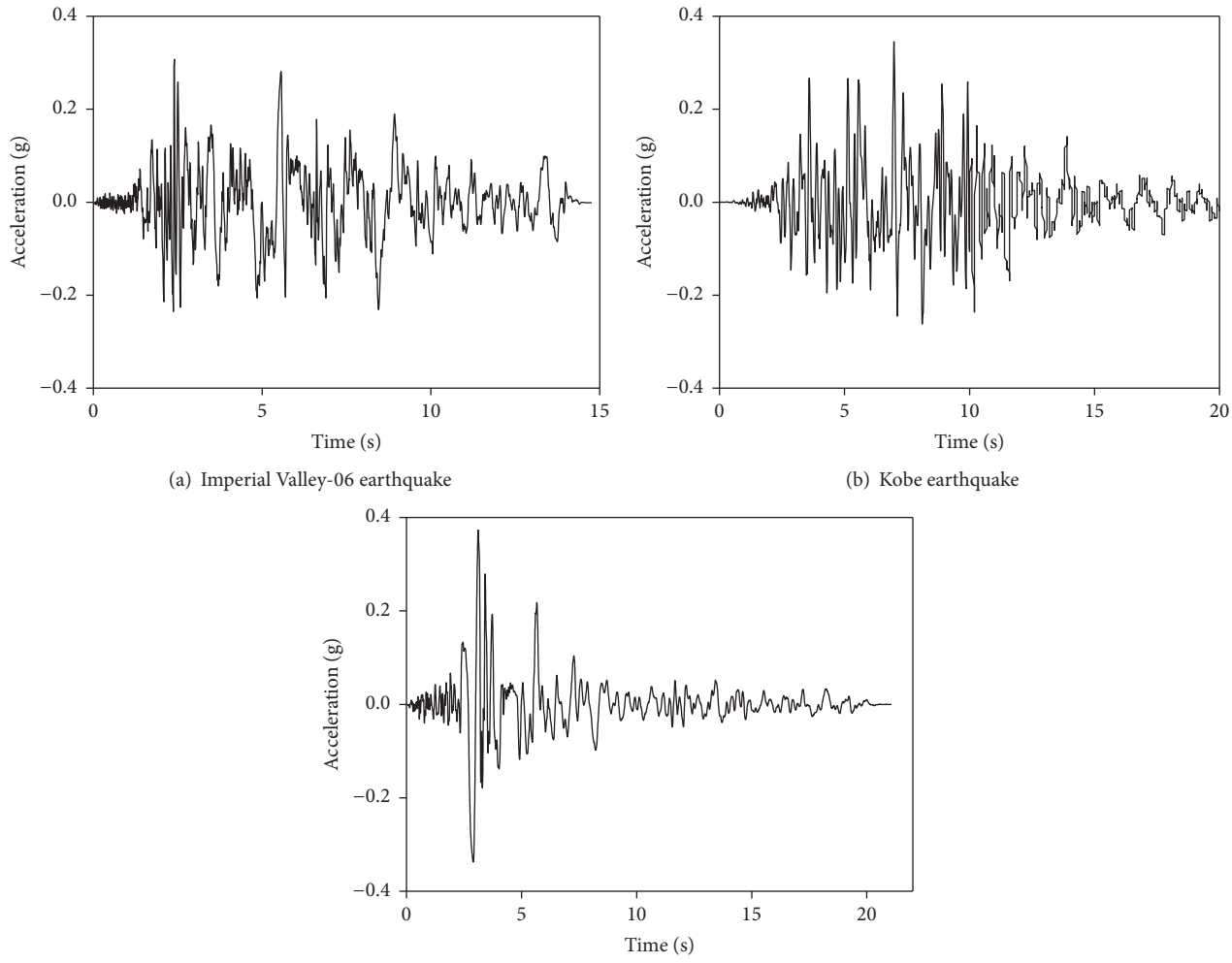

(a) Imperial Valley-06 earthquake

(b) Kobe earthquake

(c) Parkfield-02, CA earthquake

Figure 14: Acceleration records of selected earthquake.

Table 1: Results of cumulative displacement for slope A with various slope angles.

	Slope A				
Slope angle β	15°	30°	45°	60°	75°
k_c	0.155	0.135	0.115	0.107	0.046
u_x (cm)					
Imperial Valley-06	13.15	15.77	21.28	32.31	55.23
Kobe	28.35	41.45	60.46	79.49	156.43
Parkfield-02	37.45	49.14	62.23	88.78	166.45

Table 2: Results of cumulative displacement for slope B with various slope angles.

	Slope B			
Slope angle β	1 : 3	1 : 2	1 : 1	2 : 1
k_c	0.131	0.112	0.076	0.02
u_x (cm)				
Imperial Valley-06	21.84	31.44	44.89	218.88
Kobe	48.51	75.41	118.81	499.22
Parkfield-02	55.29	76.15	120.45	581.24

Acknowledgments

This research was funded by the National Natural Science Foundation of China (Grant nos. 51708405 and 51378345).

References

[1] D. G. Fredlund and J. Krahn, "Comparison of slope stability methods of analysis," *Canadian Geotechnical Journal*, vol. 14, no. 3, pp. 429–439, 1977.

[2] M. Huang and C. Song, "Upper-bound stability analysis of a plane strain heading in non-homogeneous clay," *Tunnelling and Underground Space Technology*, vol. 38, pp. 213–223, 2013.

[3] D. V. Griffiths and R. M. Marquez, "Three-dimensional slope stability analysis by elasto-plastic finite elements," *Géotechnique*, vol. 57, no. 6, pp. 537–546, 2007.

[4] I.-H. Ho, "Numerical study of slope-stabilizing piles in undrained clayey slopes with a weak thin layer," *International Journal of Geomechanics*, vol. 15, no. 5, 2014.

[5] N. M. Newmark, "Effects of earthquakes on dams and embankments," *Géotechnique*, vol. 15, no. 2, pp. 139–160, 1965.

[6] H. B. Seed, K. L. Lee, and I. M. Idriss, "Analysis of the sheffield dam failure," *Journal of the Soil Mechanics and Foundations Division, ASCE*, vol. 95, no. 6, pp. 1453–1490, 1969.

[7] H. B. Seed, "Considerations in the earthquake-resistant design of earth and rockfill dams," *Géotechnique*, vol. 29, no. 3, pp. 215–263, 1979.

[8] W. F. Chen, "Plasticity in soilmechanics and landslides," *Journal of the Engineering Mechanics Division*, vol. 106, no. 3, pp. 443–464, 1980.

[9] H. I. Ling, D. Leshchinsky, and E. B. Perry, "Seismic design and performance of geosynthetic-reinforced soil structures," *Géotechnique*, vol. 47, no. 5, pp. 933–952, 1997.

[10] R. L. Michalowski, "Soil reinforcement for seismic design of geotechnical structures," *Computers and Geotechnics*, vol. 23, no. 1-2, pp. 1–17, 1998.

[11] C.-J. Chang, W. F. Chen, and J. T. P. Yao, "Seismic displacements in slopes by limit analysis," *Journal of Geotechnical Engineering*, vol. 110, no. 7, pp. 860–874, 1984.

[12] H. I. Ling and D. Leshchinsky, "Effects of vertical acceleration on seismic design of geosynthetic-reinforced soil structures," *Géotechnique*, vol. 48, no. 3, pp. 347–373, 1998.

[13] R. L. Michalowski and L. You, "Displacements of reinforced slopes subjected to seismic loads," *Journal of Geotechnical and Geoenvironmental Engineering*, vol. 126, no. 8, pp. 685–694, 2000.

[14] X. Li, S. He, and Y. Wu, "Seismic displacement of slopes reinforced with piles," *Journal of Geotechnical and Geoenvironmental Engineering*, vol. 136, no. 6, pp. 880–884, 2010.

[15] Y. He, H. Hazarika, N. Yasufuku, Z. Han, and Y. Li, "Three-dimensional limit analysis of seismic displacement of slope reinforced with piles," *Soil Dynamics and Earthquake Engineering*, vol. 77, pp. 446–452, 2015.

[16] R. L. Michalowski, "Displacements of multiblock geotechnical structures subjected to seismic excitation," *Journal of Geotechnical and Geoenvironmental Engineering*, vol. 133, no. 11, pp. 1432–1439, 2007.

[17] M. Huang and H.-L. Qin, "Upper-bound multi-rigid-block solutions for bearing capacity of two-layered soils," *Computers and Geotechnics*, vol. 36, no. 3, pp. 525–529, 2009.

[18] D. C. Drucker, W. Prager, and H. J. Greenberg, "Extended limit design theorems for continuous media," *Quarterly of Applied Mathematics*, vol. 9, pp. 381–389, 1952.

[19] R. L. Michalowski and A. Drescher, "Three-dimensional stability of slopes and excavations," *Geotechnique*, vol. 59, no. 10, pp. 839–850, 2009.

[20] Y. Gao, S. Yang, F. Zhang, and B. Leshchinsky, "Three-dimensional reinforced slopes: evaluation of required reinforcement strength and embedment length using limit analysis," *Geotextiles and Geomembranes*, vol. 44, no. 2, pp. 133–142, 2016.

[21] F. Zhang, D. Leshchinsky, Y. Gao, and B. Leshchinsky, "Required unfactored strength of geosynthetics in reinforced 3D slopes," *Geotextiles and Geomembranes*, vol. 42, no. 6, pp. 576–585, 2014.

[22] S. Yang, B. Leshchinsky, F. Zhang, and Y. Gao, "Required strength of geosynthetic in reinforced soil structures supporting spread footings in three dimensions," *Computers & Geosciences*, vol. 78, pp. 72–87, 2016.

[23] M. Huang, H. Wang, D. Sheng, and Y. Liu, "Rotational-translational mechanism for the upper bound stability analysis of slopes with weak interlayer," *Computers and Geotechnics*, vol. 53, pp. 133–141, 2013.

[24] H. Zhou, G. Zheng, X. Yang, Y. Diao, L. Gong, and X. Cheng, "Displacement of pile-reinforced slopes with a weak layer subjected to seismic loads," *Mathematical Problems in Engineering*, vol. 2016, Article ID 1527659, 10 pages, 2016.

[25] T. Tanchaisawat, D. T. Bergado, and P. Voottipruex, "2D and 3D simulation of geogrid-reinforced geocomposite material embankment on soft Bangkok clay," *Geosynthetics International*, vol. 16, no. 6, pp. 420–432, 2009.

[26] I.-H. Ho, "Three-dimensional finite element analysis for soil slopes stabilisation using piles," *Geomechanics & Geoengineering*, 2017.